

Dehydration Is Catalyzed by Glutamate-136 and Aspartic Acid-135 Active Site Residues in *Escherichia coli* dTDP-Glucose 4,6-Dehydratase[†]

Jeffrey W. Gross,[‡] Adrian D. Hegeman,[‡] Barbara Gerratana, and Perry A. Frey*

Department of Biochemistry, University of Wisconsin–Madison, Madison, Wisconsin 53705

Received June 1, 2001; Revised Manuscript Received August 22, 2001

ABSTRACT: The dTDP-glucose 4,6-dehydratase catalyzed conversion of dTDP-glucose to dTDP-4-keto-6-deoxyglucose occurs in three sequential chemical steps: dehydrogenation, dehydration, and rereduction. The enzyme contains the tightly bound coenzyme NAD⁺, which mediates the dehydrogenation and rereduction steps of the reaction mechanism. In this study, we have determined that Asp135 and Glu136 are the acid and base catalysts, respectively, of the dehydration step. Identification of the acid catalyst was performed using an alternative substrate, dTDP-6-fluoro-6-deoxyglucose (dTDP-6FGlc), which undergoes fluoride ion elimination instead of dehydration, and thus does not require protonation of the leaving group. The steady-state rate of conversion of dTDP-6FGlc to dTDP-4-keto-6-deoxyglucose by each Asp135 variant was identical to that of wt, in contrast to turnover using dTDP-glucose where differences in rates of up to 2 orders of magnitude were observed. These results demonstrate Asp135's role in protonating the glucosyl-C6(OH) during dehydration. The base catalyst was identified using a previously uncharacterized, enzyme-catalyzed glucosyl-C5 hydrogen–solvent exchange reaction of product, dTDP-4-keto-6-deoxyglucose. Base catalysis of this exchange reaction is analogous to that occurring at C5 during the dehydration step of net catalysis. Thus, the decrease in the rate of catalysis (~2 orders of magnitude) of the exchange reaction observed with Glu136 variants demonstrates this residue's importance in base catalysis of dehydration.

Nucleotide-hexopyranose 4,6-dehydratases¹ are necessary for the biogenesis of all 6-deoxysugars, which are principle components of bacterial lipopolysaccharide, and numerous excreted secondary metabolites including many antibiotics (1–3). *Escherichia coli* dTDP-glucose 4,6-dehydratase² is one such enzyme, catalyzing the irreversible conversion of dTDP-glucose to dTDP-4-keto-6-deoxyglucose, which is further metabolized to produce components of the enterobacterial common antigen (RffG), the O-antigen repeat (RfbB), and other capsular polysaccharides (4, 5).

All 4,6-dehydratases accomplish this chemical transformation in three discrete mechanistic steps outlined in Scheme

[†] This work was supported by Grants GM30480 (P.A.F.) and GM20552 (J.W.G.) from the National Institute of General Medical Sciences.

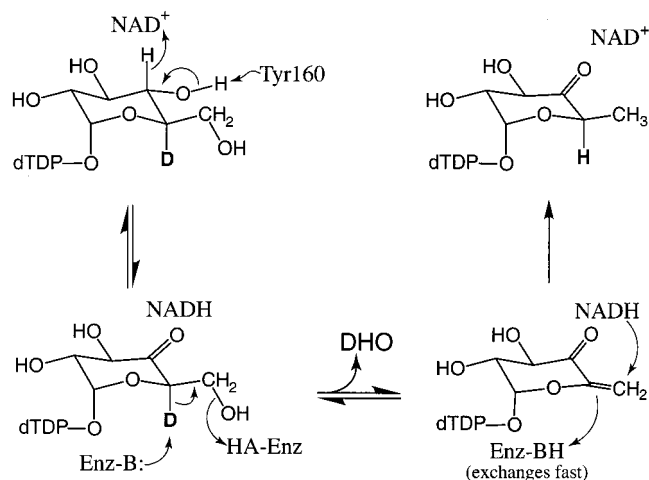
* Correspondence should be addressed to this author at the University of Wisconsin–Madison, 1710 University Ave., Madison, WI 53705. Tel: (608) 262-0055. Fax: (608) 265-2904. E-mail: frey@biochem.wisc.edu.

[‡] Both authors have contributed equally to this work.

¹ Abbreviations: BSA, bovine serum albumin; DMF, *N,N*-dimethylformamide; 4,6-dehydratase, dTDP-glucose 4,6-dehydratase; dTDP-glucose, thymidine 5'-diphospho- α -D-glucose; dTDP-glucose-*d*₇, dTDP-[1,2,3,4,5,6,6-²H₇]glucose; dTDP-6FGlc, dTDP-6-deoxy-6-fluoroglucose; dTDP-4-keto-6-deoxyglucose-5-*d*₁, dTDP-4-keto-6-deoxy-[5-²H]glucose; dTDP-xylose-5-*d*₁, dTDP- α -D-[5-²H]xylose; DTT, dithiothreitol; dTTP, thymidine 5'-triphosphate; EDTA, ethylenediaminetetraacetic acid; HEPES, 4-(2-hydroxyethyl)piperazine-1-ethanesulfonic acid; MALDI-TOF MS, matrix-assisted laser desorption/ionization time-of-flight mass spectrometry; NAD⁺, nicotinamide adenine dinucleotide (oxidized); NADD, [4-²H₁]nicotinamide adenine dinucleotide (reduced); NADH, nicotinamide adenine dinucleotide (reduced); NMR, nuclear magnetic resonance; TRIS, tris(hydroxymethyl)aminomethane; wt, wild type.

² dTDP α -D-glucose 4,6-hydro-lyase, EC 4.2.1.46.

Scheme 1



1 (reviewed in 6). In the first step, dehydrogenation, a hydride is transferred from the glucosyl C4 to NAD⁺ (tightly bound), with deprotonation of the C4(OH) to form dTDP-4-ketoglucose. After formation of the 4-ketone, the pK_A of the C5(H) is significantly decreased, facilitating the second step, dehydration. This step requires base catalysis for abstraction of the C5(H) and acid catalysis for protonation of the leaving C6(OH). In the third and final step in the mechanism, the dTDP-4-ketoglucose-5,6-ene is reduced, as hydride is transferred from NADH to glucosyl C6, and C5 is reprotonated.

In recent structural and mechanistic studies of *E. coli* RffG (7) and *Salmonella enterica* RmlB (8), attempts have been made to assign active site residues to the catalysis of these

three steps. Base catalysis of the dehydrogenation step has been shown to be accomplished in RffG by the Tyr160 tyrosinate anion ($pK_A = 6.4$; 9). This tyrosine belongs to one of the signature motifs (YXXXX) of the short-chain dehydrogenase/reductase superfamily (10) and has been shown to be the base catalyst for dehydrogenation in a closely related family member, UDP-galactose 4-epimerase (11). Assignment of residues catalyzing the second and third steps of the mechanism has been ambiguous. Candidates for catalysis of the second and third steps include Asp135, Glu136, and Tyr301. These three residues reside proximal to the C6–C5, and variants of these residues have been shown to have significant effects on the overall catalytic rate, while not altering catalysis of the dehydrogenation step (7). Heretofore, there has been no biochemical evidence supporting the participation of any given active site residue in the catalysis of dehydration. This is mostly because the complexity of the 4,6-dehydratase reaction makes it difficult to assign the effects of mutagenesis on the overall reaction to specific chemical steps.

Here, we describe two new approaches that have been developed to specifically evaluate the effects of active site variants on the dehydration step. The first uses MALDI-TOF MS to determine the kinetics of solvent hydrogen exchange from C5 of the deuterated product, dTDP-4-keto-6-deoxyglucose-*d*₇. Although complete exchange from C5 occurring during net catalysis is well documented (Scheme 1; 12, 13), the product exchange has never been reported. Second, we have synthesized a novel substrate analogue, dTDP-6FGlc. This compound eliminates H⁺ and F⁻, rather than H₂O, during the second step in the reaction, thus removing the need for acid catalysis while still requiring base catalysis.

EXPERIMENTAL PROCEDURES

Methods and Materials. Wt and variant 4,6-dehydratases were prepared using the affinity purification procedure outlined previously; all of the variants studied herein were shown previously to have identical molar ellipticity circular dichroism spectra to wt (7). Dry pyridine, acetic anhydride, crystalline H₃PO₄, and dTTP were obtained from Aldrich. Inorganic pyrophosphatase was purchased from Boehringer Mannheim. UDP-glucose pyrophosphorylase and 6-deoxy-6-fluoroglucose were from Sigma. Synthesis and purification of dTDP- α -D-glucose and dTDP- α -D-glucose-*d*₇ and analysis of samples by MALDI-TOF MS were performed as described previously (14). Mass spectra were collected on a PE-Biosystems Voyager-DE MALDI-TOF mass spectrometer, equipped with delayed extraction, in the negative-ion reflectron mode. Enzyme and nucleotide-sugar concentrations were determined using UV/Visible measurements with a Shimadzu UV-1601PC dual beam spectrophotometer or a Hewlett-Packard 8452A diode array spectrophotometer and extinction coefficients of 81 000 M⁻¹ cm⁻¹ for enzyme and 10 200 M⁻¹ cm⁻¹ for thymidine nucleotides, both at pH 7.0, 20 °C. A Beckman LS 6500 multipurpose scintillation counter was used to quantify radioactivity.

Determination of Product Dissociation Constant. The K_D for product binding to wt 4,6-dehydratase was determined by equilibrium ultrafiltration (15). For this analysis, radiolabeled product was produced enzymatically in unbuffered H₂O, using 4,6-dehydrase to convert [β -³²P]dTDP-glucose

(7) to [β -³²P]dTDP-4-keto-6-deoxyglucose. Following complete conversion to product, the enzyme was removed by ultrafiltration (Microcon-10, Amicon). Binding reactions (200 or 250 μ L) consisted of 4,6-dehydratase (1.14–250 μ M) and radiolabeled product (2.4–500 μ M) in 100 mM TRIS-HCl, pH 7.5, 1 mM EDTA. The reactions were preincubated for 10 min at room temperature; then representative portions of the free ligand were isolated by passage through Microcon-10 ultrafiltration units (14000g for 1–5 min). Radioactivity in aliquots of the initial binding reaction and of the ultrafiltration permeate was quantified by liquid scintillation counting. Data were corrected for 60% radio-purity of the [β -³²P]dTDP-4-keto-6-deoxyglucose, and, with the permeate, for 4% nonspecific binding of the radioligand to the ultrafiltration membrane. The corrected values were then used to calculate the concentration of free ligand, [L_{free}], and the concentration of enzyme-bound ligand, [EL], for each binding reaction. The data were fitted (Kaleidagraph, Synergy Software, using the Levenberg–Marquardt algorithm) to the equation: $[EL]/[E_{total}] = n([L_{free}]/([L_{free}] + K_D))$, yielding a K_D value of $24.7 \pm 5.0 \mu$ M, and 1.06 ± 0.05 ligand binding sites per subunit.

Deuterium Labeled Product. dTDP-4-keto-6-deoxyglucose-*d*₇ and dTDP-4-keto-6-deoxyglucose-5-*d*₁ were generated enzymatically from dTDP-glucose-*d*₇ and unlabeled dTDP-glucose with 4,6-dehydratase in D₂O in the absence of buffer, salt or DTT, at 20 °C. Enzyme, 0.25 mM, in 10 mM MOPS, pH 7.0, and 1 mM DTT was exchanged into D₂O by passing it through two D₂O-equilibrated G-50 (Pharmacia), 1 mL centrifuge columns (16). dTDP-glucose was exchanged into D₂O by lyophilizing, redissolving the solid in D₂O, lyophilizing again, and dissolving the sample in D₂O once more. The exchanged dTDP-glucose and 4,6-dehydratase samples were combined, and dTDP-4-keto-6-deoxyglucose formation was monitored spectrophotometrically using the Okazaki method (17). Once all of the substrate was converted to product, enzyme was removed by ultrafiltration (Microcon-10, Amicon), and the filtrate, containing the C5(D)-product, was lyophilized and resuspended in H₂O. Following an additional round of lyophilization and resuspension in H₂O, product concentration was determined spectrophotometrically using the above extinction coefficient for thymidine nucleotides. Deuterium enrichment at C5 for dTDP-4-keto-6-deoxyglucose-*d*₇ and dTDP-4-keto-6-deoxyglucose-5-*d*₁ was determined by MALDI-TOF MS to be 86% for both species.

Deuterium Labeled dTDP-Xylose. Synthesis of dTDP-xylose-5-*d*₁ was accomplished enzymatically as described for product, but reaction progress was followed by ¹H NMR spectrometry (200 MHz, Bruker). The reaction was monitored over 4 days until complete as judged by the decrease in the integration for the secondary multiplet from 3.5 to 3.8 ppm (assigned to C2, C3, C4, and two C5 protons) from 5 to 4 protons. Only one of the two C5 protons exchanged over 4 days. The final isotopic enrichment was found to be 92% by MALDI-TOF MS.

Product and dTDP-Xylose Exchange Reactions. MALDI-TOF MS was used to quantify the 4,6-dehydratase-catalyzed exchange of protium for deuterium at glucosyl-C5 of dTDP-4-keto-6-deoxyglucose-*d*₇, dTDP-4-keto-6-deoxyglucose-5-*d*₁, or dTDP-xylose-5-*d*₁ in quenched samples. Reactions were initiated by addition of enzyme, and were performed

in H₂O at 18 °C with saturating dTDP-4-keto-6-deoxyglucose (1 mM, $K_D \sim 25 \mu\text{M}$) or dTDP-xylose (1 mM, $K_I \sim 11 \mu\text{M}$) in 10 mM NH₄OAc, 1 mg/mL BSA (fraction V), and 1 mM DTT, adjusted to a pH of 7.5 with NH₄OH. All of the variants have a remarkable absence of K_M effects with the natural substrate (7; changes in product release rates will typically be manifest in K_M in addition to those in substrate binding and other post-committed catalytic steps). It was assumed that the variants would have within 10-fold K_D values for product as wt, and so 1 mM product would be more than sufficient to maintain saturating conditions. Aliquots (10 μL) were quenched at various time points (from 2 min to 48 h) by addition to 100 μL of ethanol at 65 °C. Quenched samples were vortexed and placed on ice prior to centrifugation to remove precipitated protein. Supernatant was transferred to new tubes and concentrated to dryness in vacuo in a Speed-Vac Concentrator (Savant). The resulting residue was resuspended in 6 μL of water and analyzed by MALDI-TOF MS as described previously (14). Control experiments containing no enzyme were performed, and showed no detectable exchange over the same time range used for the enzyme-catalyzed reactions. The extent of glucosyl C5(D) solvent proton exchange was plotted vs time and fitted to a single exponential (Kaleidagraph, Synergy Software, using the Levenberg–Marquardt algorithm). The single exponential value [mM product (or dTDP-xylose) · s⁻¹] was divided by the enzyme concentration (mM) to give the rate constant for exchange (s⁻¹).

The pH dependence of product exchange was determined using the previously described piperazine/HEPES/KCl buffer system (7) supplemented with 1 mg/mL BSA (fraction V) and 1 mM DTT. The reactions were incubated and quenched as above, except that the quenched samples were desalted using 1 mL Toyopearl HW-40S (TOSOHAAS) centrifuge columns (16). For this procedure, protein-free samples were concentrated to near dryness and resuspended in 180 μL of H₂O prior to being loaded onto the column. The columns were centrifuged at 1100g for 2 min, and the flow-through (containing product) was concentrated to $\sim 10 \mu\text{L}$ prior to MALDI-TOF analysis, as above.

dTDP-6FGlc. Solid 6-deoxy-6-fluoro-D-glucose (275 μmol) was dissolved in 1 mL of dry pyridine and peracetylated by reaction with excess (2.12 mmol) acetic anhydride (4 °C, 12 h, stirred under dry N₂). Pyridine and unreacted acetic anhydride were removed by rotary evaporation. The resulting syrup was dissolved in chloroform and contaminating pyridinium acetate removed by treatment with prewashed (chloroform) mixed-bed ion-exchange resin (Bio-Rad, RG 501-X8). Chloroform was removed from the treated solution in vacuo, and the acetylation stoichiometry (four acetate groups per pyranose) was confirmed by ¹H NMR spectrometry in deuteriochloroform.

The tetraaceto-6-deoxy-6-fluoroglucose was dried at reduced pressure in a desiccator over P₂O₅ and subsequently phosphorylated at carbon 1 by the MacDonald procedure (18). Crystalline H₃PO₄, 1.1 mmol, was mixed with the tetraaceto-6-deoxy-6-fluoroglucose in a flask maintained under vacuum and stirred at 50 °C. After 2 h, the reaction was cooled to room temperature and removed from the vacuum line, and then 5 mL of 2 M LiOH was added at room temperature to hydrolyze the acetate esters and to precipitate unreacted phosphate. Saponification proceeded

for 16 h at room temperature, at which point precipitated Li₃PO₄ was removed by centrifugation. The Li₃PO₄ pellet was washed with 0.01 M LiOH and subjected to centrifugation. The combined supernatants were chilled on ice and passed through a cation exchange column in the H⁺ form (Bio-Rad RG 50W-X8) at 4 °C. The acidic flow-through (pH 3) was rapidly adjusted to pH 7.2 with NH₄OH and then lyophilized. The 6-deoxy-6-fluoroglucose-1-phosphate was dissolved in D₂O and found to be predominantly (>90%) the α -anomer by ¹H NMR spectrometry (dd, 5.3 ppm as in α -D-glucose-1-phosphate). The ³¹P NMR spectrum showed two peaks at -1.9 (10%) and -2.3 ppm (90%) (0 ppm set to 85% H₃PO₄ standard) with peak volumes consistent with the β - and α -anomers, respectively.

The dTDP-6FGlc synthesis was completed enzymatically by coupling the sugar-1-phosphate to dTTP using UDP-glucose pyrophosphorylase. The 1 mL reaction mixture contained half of the 6-fluoroglucose-1-phosphate from the previous step, 50 units of UDP-glucose pyrophosphorylase, 4 units of inorganic pyrophosphatase, 10% glycerol, 1 mM DTT, 100 mM TRIS-HCl, pH 7.5, 12 mM MgSO₄, and 10 mM dTTP. The reaction was incubated at 20 °C and monitored (treatment with 4,6-dehydratase followed by the Okazaki assay; 17) for 2 days after which the reaction was supplemented with an additional 10 μmol each of dTTP and MgSO₄. The reaction was monitored for an additional 2 days with minimal additional product formation and was subsequently terminated by removing protein (ultrafiltration Microcon-10, Amicon). The permeate was loaded onto a 8 mL Mono-Q column (acetate form) and eluted with a 50 mL linear NH₄OAc gradient from 10 to 500 mM. The dTDP-6FGlc was desalted by gel filtration (TOSOHAAS Toyopearl HW-40S, 120 mL) in H₂O at 1 mL/min flow rate and lyophilized. A final yield of 10 μmol of dTDP-6FGlc was obtained after purification; the monoanionic mass was confirmed by MALDI-TOF MS to be m/z 565.2 (M-H).

dTDP-6FGlc Turnover. The conversion of dTDP-6FGlc into dTDP-4-keto-6-deoxyglucose by 4,6-dehydratase was followed by spectrophotometric detection of a product-derived chromophore at 318 nm (17). Reaction rates for wt and variant 4,6-dehydratases were determined in pH 7.5 TRIS-HCl, 1 mg/mL BSA fraction V, and 1 mM DTT, at 37 °C. A complete steady-state analysis was performed with wt enzyme with dTDP-6FGlc concentrations bracketing the K_M ; rate data were fitted to the Michaelis–Menten equation to yield k_{cat} and k_{cat}/K_M (Kaleidagraph, Synergy Software, using the Levenberg–Marquardt algorithm). The turnover rates for variant 4,6-dehydratases were measured at saturating concentrations of dTDP-6FGlc. Saturating conditions were verified by measuring turnover at two dTDP-6FGlc concentrations (2 and 3 mM). In all cases, these values were identical within error and thus representative of k_{cat} for each mutant enzyme.

RESULTS

Identification of active site residues involved in specific catalytic steps is complicated by the complexity of the 4,6-dehydratase chemical mechanism. Numerous active site residues have been identified as being important for catalysis, but only through the analysis of the reaction of a substrate analogue (dTDP-xylose) has the extent of each variant's

Table 1: Saturation Kinetic Parameters for Product C5 Exchange and dTDP-6FGlc Turnover Reactions with Wt and Variants

	dTDP 4-keto-6-deoxyglucose- <i>d</i> ₇ C5(H/D) exchange		dTDP-6FGlc turnover ^d		dTDP-glucose turnover ^c	
	k_{exch} (s ⁻¹)	$-\Delta^b$	k_{cat} (s ⁻¹)	$-\Delta^b$	k_{cat} (s ⁻¹)	$-\Delta^b$
wt	0.12	1	0.044	1	4.9	1
D135A	0.24	0.5	0.029	1.5	0.022	223
D135N	0.35	0.3	0.053	0.8	0.0395	124
D135N/E136Q	0.0008	150	0.00013	340	0.024	204
E136A	0.001	120	0.000064	690	0.017	288
E136Q	0.0031	39	0.00064	69	0.073	67
Y301F	0.011	11	0.0014	31	0.042	117
K199R	0.00052	230	0.000065	680	0.017	288
K199M	0.0013	92	0.00017	260	0.0425	115
E198Q	0.00039	310	0.00023	190	0.019	258

^a Values represent the average of two measurements taken at saturating substrate concentrations. ^b “ $-\Delta$ ” refers to the fold change below the rate listed for wt. In a few cases, the number is less than 1, indicating that the variant catalyzes the process faster than wt. ^c The values in this column have been previously reported (7).

effects on a subportion of the reaction (the dehydrogenation step) been evaluated (7, 9). In this study, we introduce two 4,6-dehydratase-catalyzed reactions that can be used to evaluate the effects of variants on the dehydration chemistry: C5(H) exchange of the product dTDP-4-keto-6-deoxyglucose with solvent; and the conversion of dTDP-6FGlc into dTDP-4-keto-6-deoxyglucose.

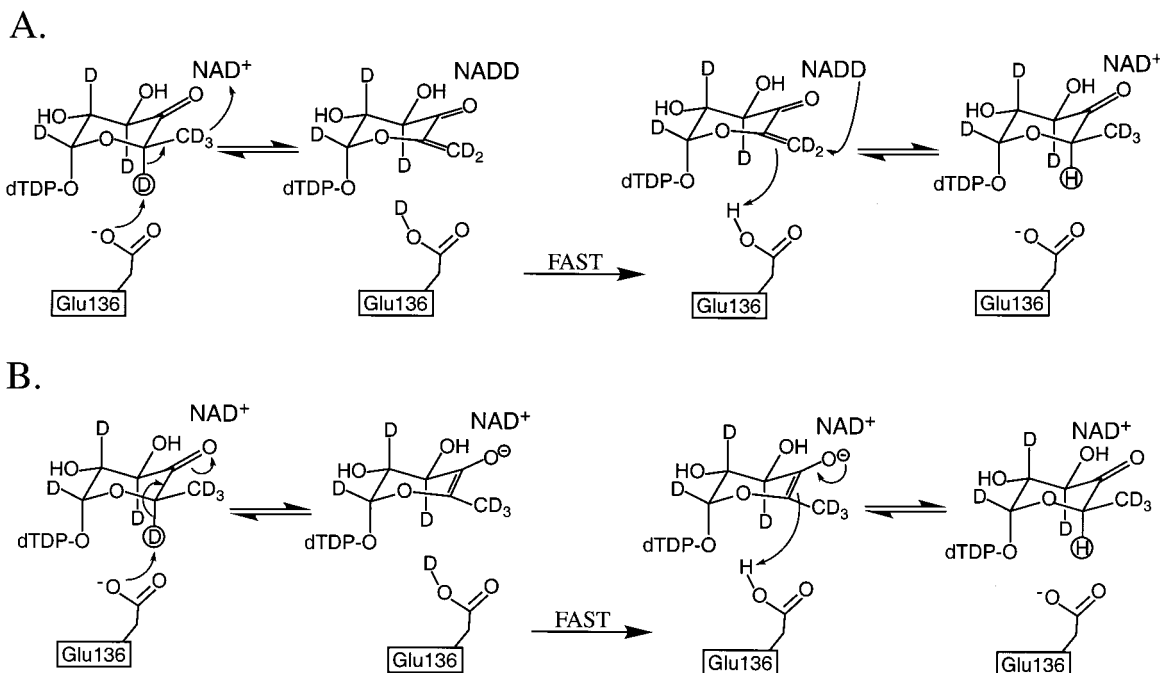
Product C5 Solvent Hydrogen Exchange. To identify active site residues participating in base catalysis of glucosyl-C5 solvent hydrogen exchange, an investigation of the rates of this exchange from dTDP-4-keto-6-deoxyglucose-*d*₇ catalyzed by wt and variant 4,6-dehydratase was initiated. The rate constants for deuterium to hydrogen exchange (k_{exch}) were determined as described under Experimental Procedures for wt and nine previously constructed 4,6-dehydratase active site residue variants (7), and are listed in Table 1. While the nature of this exchange chemistry will be dealt with exten-

sively below, it is likely that the only catalytic participant in the exchange common to the physiological reaction is the base that abstracts the C5 proton during water elimination.

The Asp135 single residue variants' k_{exch} values were similar to wt (or slightly larger). The Y301F variant was only 11-fold slower than wt, while the Glu136 variants, including the D135N/E136Q double variant, ranged between 39- and 150-fold below wt. These results support the assignment of Glu136 as the residue that abstracts the C5(H) during water elimination and reprotonates C5 during dTDP-4-ketoglucose-5,6-ene reduction. The low k_{exch} values for the Glu198 and Lys199 variants, given earlier observations, suggest a different function for these residues. To date, in every type of analysis employed—including the kinetics of the reactions of dTDP-glucose and dTDP-xylose apart from C5(H) exchange of the product and reaction of dTDP-6FGlc—the Glu198 and Lys199 variants have demonstrated large negative consequences for catalysis. Structural evidence does not indicate appropriate placement of either of these residues for direct participation in acid/base chemistry (see Discussion). The simplest explanation for these observations is that modification of Glu198 or Lys199 brings about misalignments of the pyranose in its subsite, which alter productive interactions between the pyranose and catalytic residues.

Product Exchange Isotope Effects. The product exchange reaction likely occurs by one of two mechanisms. The first involves catalysis in the reverse direction, and would minimally require both proton abstraction at C5 and hydride transfer from C6 to NAD⁺, forming NADH and the dTDP-4-ketoglucose-5,6-ene intermediate (see Scheme 2A). If exchange occurs by this mechanism, using our single turnover results, we predict that about 10% of the enzyme should be in the NADH form (14). Accordingly, we should be able to observe NADH spectrophotometrically by saturating wt with product. We were unable to detect NADH during this reaction, but because the equilibrium for this reaction

Scheme 2



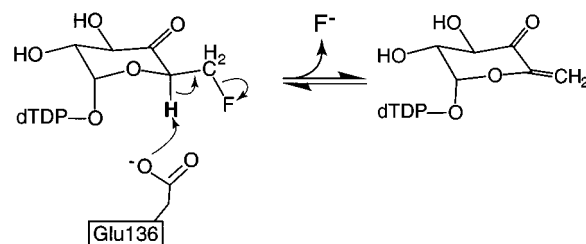
may favor product more than anticipated, we cannot exclude this mechanism on the basis of a negative result. The second mechanism involves base-catalyzed enolization of the product, followed by solvent exchange from the enzyme base, and reketonization (Scheme 2B).

To test whether the product exchange reaction proceeds through reversal of catalysis, exchange rates with dTDP-4-keto-6-deoxyglucose-*d*₇ and dTDP-4-keto-6-deoxyglucose-5-*d*₁ were determined. Because catalysis in the reverse direction requires hydride transfer from C6, this reaction would display a primary deuterium kinetic isotope effect; thus, a considerably slower exchange rate (2–8-fold) for the dTDP-4-keto-6-deoxyglucose-*d*₇ would be expected. Rate measurements (quadruplicate) with dTDP-4-keto-6-deoxyglucose-*d*₇ and dTDP-4-keto-6-deoxyglucose-5-*d*₁ were used to determine $^Dk_{\text{exch}} = 1.25 (\pm 0.12)$. This small isotope effect, near unity, indicates that no carbon–hydrogen-bond cleavage occurs at C6. It is unlikely that a larger isotope effect is being masked by other steps, as product release is clearly not rate-limiting in the much faster physiological reaction, enzyme is clearly saturated with product, and active site base–solvent hydrogen exchange is much faster than product release (7, 14). From these results, we conclude that product C5(H) solvent exchange occurs by the enolization mechanism (Scheme 2B).

dTDP-Xylose C5 Solvent Hydrogen Exchange. The rates of solvent hydrogen exchange at dTDP-xylose C5 were found to be 0.001, 0.002, and 0.00007 s⁻¹ for wt and variants D135A and Y301F, respectively. This exchange could not be detected with other variants, and must be occurring at a rate slower than 0.00001 s⁻¹, our lower limit of detection. It is interesting that wt-catalyzed exchange from dTDP-xylose occurs in excess of 2 orders of magnitude slower than from the product, dTDP-4-keto-6-deoxyglucose. As C5 exchange can only occur from a 4-ketosugar, one might expect the dTDP-xylose exchange to be only slightly slower than product exchange, given that as much as 73% of the bound dTDP-xylose is oxidized to the 4-ketone in the active site under saturating conditions (7). The extraordinarily slow C5 exchange rate may help resolve results from our previous work (7) where investigation of the extent of oxidation of dTDP-6-deoxyglucose revealed 10-fold lower levels (7–8% of the 4-ketone/NADH) of NADH formed than with dTDP-xylose (under identical reaction conditions). The dTDP-4-ketoxylose apparently slips into a nonproductive complex, resulting in slowed C5 exchange rates and a 10-fold shift in the redox equilibrium.

dTDP-6FGlc Turnover. The analysis of the 4,6-dehydratase reaction with dTDP-6FGlc is central to our investigation of the acid catalysis of the dehydration step. This substrate analogue is converted to the same product (dTDP-4-keto-6-deoxyglucose) as is the physiological substrate except that it proceeds through the release of fluoride ion and H⁺ rather than water (Scheme 3), as confirmed by mass spectrometric and spectrophotometric evidence. Interestingly, a similar compound, CDP-6-difluoro-6-deoxyglucose, was designed as a mechanism-based inactivator of a related enzyme, CDP-glucose 4,6-dehydratase (19); the enzyme is capable of catalyzing the elimination of both fluorine atoms prior to forming a covalent adduct with the resulting electrophile. While fluorine is clearly a functional substitution for the C6(OH), it also obviates the need for acid catalysis

Scheme 3



for the elimination chemistry. The steady-state parameters for turnover of dTDP-6FGlc by wt 4,6-dehydratase are $k_{\text{cat}} = 0.044 (\pm 0.005) \text{ s}^{-1}$, $k_{\text{cat}}/K_M = 160 (\pm 40) \text{ M}^{-1} \text{ s}^{-1}$, and $K_M = 0.274 (\pm 0.098) \text{ mM}$. These values show significant differences from the parameters determined under the same conditions with dTDP-glucose ($k_{\text{cat}} = 4.9 \text{ s}^{-1}$, $k_{\text{cat}}/K_M = 820\,000 \text{ M}^{-1} \text{ s}^{-1}$, and $K_M = 0.0060 \text{ mM}$; 7). Values of k_{cat} and k_{cat}/K_M show 110- and 5125-fold decrements, and the K_M value is 46-fold larger.

The rates of turnover were determined for nine active site variants (Table 1). These data support the assignment of the acid catalyst for dehydration to Asp135. Variants of Asp135 are the only ones that do not show a significantly slower rate of dTDP-6FGlc turnover than wt. The Asp135 variants show little effect on the first step in catalysis, as shown with dTDP-xylose, but 124–223-fold decrements in k_{cat} with dTDP-glucose (7). We propose that the lowered activity in the physiologically relevant reaction with these variants is due to the absence of Asp135's acid catalysis of elimination, which is not required in the reaction with dTDP-6FGlc.

dTDP-6FGlc was used to check for the formation of two intermediates that had been detected with authentic substrate during net catalysis: C5-exchanged substrate, which accumulated to constitute 20% of total substrate during net turnover, and NADH, which accounts for 45% of total enzyme during steady-state turnover. To assay for C5-exchanged substrate, catalysis was performed in D₂O, quenched in 65 °C ethanol and followed by MALDI-TOF MS as per product C5 exchange reactions (see Experimental Procedures). Only dTDP-6FGlc ($m/z = 565.2 \text{ M-H}$) and dTDP-4-keto-6-deoxyglucose-5-*d*₁ ($m/z = 565.2 \text{ M-H}$) were observed. Unlike the reaction with dTDP-glucose, no reaction intermediates, having exchanged C5(H), or eliminated 6F, could propagate back into substrate and generate either dTDP-6-F-glucose-5-*d*₁ or dTDP-glucose, respectively. Similar to the reaction with authentic substrate, the C5(H) exchange from dTDP-6FGlc during net catalysis is complete. Second, to determine the extent of NADH formation during steady-state turnover of dTDP-6FGlc, 0.1 mM wt 4,6-dehydratase and 6.7 mM dTDP-6FGlc were combined in 100 mM TRIS-HCl, pH 7.5, 1 mM DTT, and 1 mg/mL BSA fraction V, and observed spectrophotometrically. No detectable NADH was formed during this reaction; the theoretical ΔA_{340} for 100% NADH formation is estimated to be 0.6 OD unit ($\epsilon_{340\text{NADH}} = 6 \text{ mM}^{-1} \cdot \text{cm}^{-1}$).

The pH dependencies of both the product C5 solvent hydrogen exchange and dTDP-6FGlc turnover reactions were also analyzed. For both of these reactions, the pH and ionic strength were maintained using the piperazine/HEPES/KCl buffer system described previously (7). The log of the constant for the observed rate of catalysis, k_{obs} , was plotted vs pH (Figure 1). The $\text{p}K_A$ values were derived by nonlinear

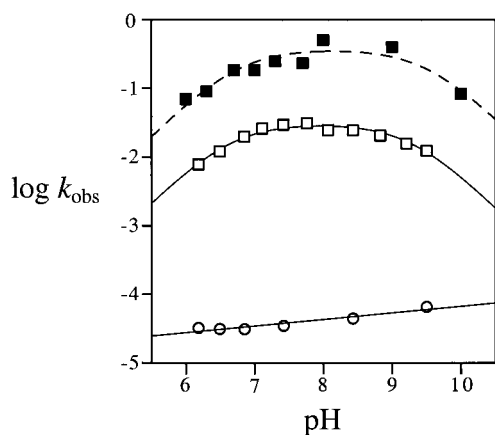


FIGURE 1: pH dependence of product C5 exchange and dTDP-6FGlc turnover. Product C5 exchange data for wt 4,6-dehydratase (\square) are shown with the dashed fitted line derived by fitting the data to the equation from the BELL program (20). dTDP-6FGlc turnover data for wt (\blacksquare) and E136A (\circ) are shown with solid lines derived by fitting data to the BELL equation and by linear regression, respectively.

fitting of k_{obs} data to the equation for a bell-shaped pH profile [$y = \log(c/(1 + 10^{(\text{pH}-\text{p}K_{\text{A}1})}) + 10^{(\text{p}K_{\text{A}2}-\text{pH}))})$ where c is a constant; 20].

E136A-catalyzed dTDP-6FGlc turnover is largely pH-independent; k_{obs} data were fitted to a straight line that increases slightly with pH (slope = 0.095, intercept = -5.1, $R = 0.95$). Wt displays a bell-shaped pH dependence for dTDP-6FGlc turnover with $\text{p}K_{\text{A}1}^{\text{dTDP-6FGlc}} = 6.63 (\pm 0.06)$ and $\text{p}K_{\text{A}2}^{\text{dTDP-6FGlc}} = 9.29 (\pm 0.06)$. The pH dependence for wt 4,6-dehydratase product C5 exchange was also bell-shaped with $\text{p}K_{\text{A}1}^{\text{exch}} = 6.76 (\pm 0.17)$ and $\text{p}K_{\text{A}2}^{\text{exch}} = 9.51 (\pm 0.21)$. Both the wt and E136A reactions with dTDP-6FGlc were performed with 2 mM nucleotide-sugar over the pH range. Saturating conditions were tested by repeating the measurements with 3 mM dTDP-6FGlc at pHs 6.18, 7.5, and 9.5 for wt and E136A. Each rate was identical within error to its counterpart determined at 2 mM except that measured at pH 9.5 for E136A, which was significantly faster. Saturating conditions were similarly tested and verified for the product C5 exchange at pH 6.

DISCUSSION

The principal goal of this investigation was to identify the active site residues responsible for the acid-base catalysis of dehydration by 4,6-dehydratase. Compelling evidence leads us to conclude that Glu136 is the base and Asp135 is the acid, which catalyze water elimination, and that Glu136 also reprotonates C5 during the reduction of the dTDP-4-ketoglucose-5,6-ene. In our previous studies, variants of Asp135 and Glu136 displayed significant effects on the turnover of dTDP-glucose, yet did not appear to affect the catalysis of the initial dehydrogenation step (7). Our homology model of the 4,6-dehydratase active site shows that Asp135 and Glu136 are on the correct side of the active site to be interacting with the C6(OH) and the C5(H). These predictions have been buoyed by crystallographic data and models, which suggest that Glu136 may be close to the C5 proton and that Asp135 is near the C6(OH) (8). Homologous glutamate residues have been predicted to function as the base catalyst of dehydration in *Salmonella enterica* dTDP-

glucose 4,6-dehydratase (RmlB; 21) and *E. coli* GDP-mannose 4,6-dehydratase (22).

The fact that the Asp135 variants catalyze turnover of dTDP-6FGlc at a rate comparable to wt indicates that whatever function Asp135 has in the dTDP-glucose reaction is not needed in the dTDP-6FGlc reaction. This function is most likely protonation of the leaving group, which is needed for water elimination but not for fluoride elimination. Glu136 variants have large effects on the rate of dTDP-6FGlc turnover, which is consistent with Glu136 being the base catalysts. The pH dependence of dTDP-6FGlc turnover with wt indicates a requirement for a deprotonated species with a $\text{p}K_{\text{A}1}^{\text{dTDP-6FGlc}} = 6.63 (\pm 0.06)$. This dependence is absent in the E136A profile, further supporting the assignment of a deprotonated Glu136 acting as the base catalyst for fluoride elimination.

Glu136 variants show significant effects on the product C5 solvent hydrogen exchange rates, identifying Glu136 as the acid-base catalyst of this process. With wt, the pH dependence of product C5 exchange shows a $\text{p}K_{\text{A}1}^{\text{exch}} = 6.76 (\pm 0.17)$, which is the same, within error, as that seen in the dTDP-6FGlc reaction (immediately above). Given Glu136's role in this exchange reaction, it is probably similarly employed for C5 proton abstraction and reprotonation in the turnover of dTDP-glucose.

Previous studies showed that Tyr160 is responsible for removing the C4(OH) proton during the first step in catalysis, dehydrogenation of substrate (9). Dehydrogenation is clearly rate-limiting for the Y160F variant, which has a k_{cat} that is 2 orders of magnitude lower than that of wt. The pH profile of k_{cat} for Y160F exhibits an acid-side $\text{p}K_{\text{A}}$ of 6.6, which was originally assigned to either Glu136 or Asp135 as potential surrogates for Tyr160. Our current studies suggest that the Glu136 is indeed acting as the surrogate base with a $\text{p}K_{\text{A}}$ of 6.6 in Y160F. Such catalytic promiscuity helps to explain why single-residue active site variants of 4,6-dehydratase display only 2 orders of magnitude lower activity while 4 or 5 orders of magnitude lower activity might be expected.

While Glu198 and Lys199 variants also display significantly slower rates of dTDP-6FGlc turnover and product C5 solvent hydrogen exchange, they do not participate directly in chemical catalysis, but are instead important for the productive positioning of the pyranose moiety in the active site. Both our homology model and the RmlB structure show that the Glu198 and Lys199 are located on the wrong side of the pyranose binding pocket to interact with the C5(H) and C6(OH); as shown in Figure 2, they are situated near the C2(OH) and the oxygen atoms of the β -phosphate (8). In addition, all of the Glu198 and Lys199 variants show 2–3 orders of magnitude lower rates than wt for every reaction thus far characterized including turnover of dTDP-glucose, and approach to equilibrium with dTDP-xylose, in addition to dTDP-6FGlc turnover and the exchange reaction (7). Since the rates of each of these processes are controlled by different 4,6-dehydratase catalytic elements, the observed effects cannot be assigned to removal of a particular acid or base catalyst. Instead we must look for a common element, which in this case is the formation of a productive pyranose-active site complex. Variants of Glu198 and Lys199 must misalign the sugar in the active site so that the rate of chemistry is,

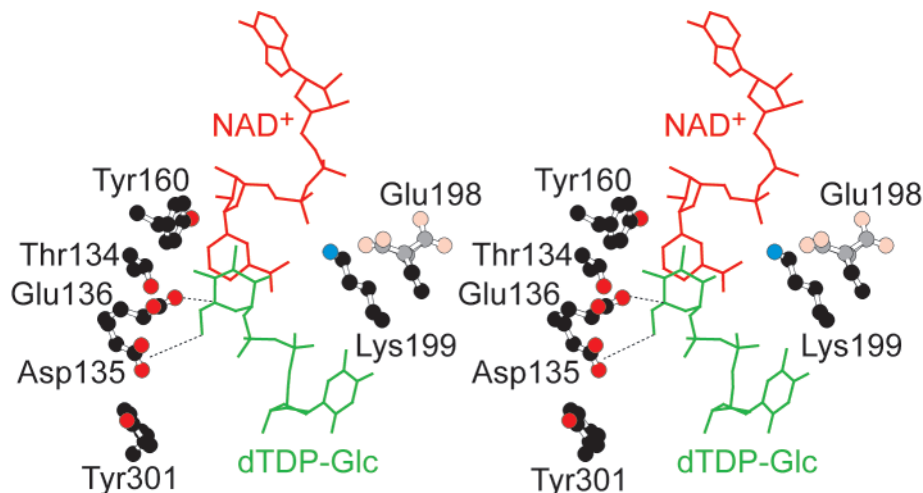


FIGURE 2: Stereoview of a 4,6-dehydratase/NAD⁺/dTDP-glucose active site model. The dTDP-glucose was placed in the 4,6-dehydratase active site (PDB file 1BXK) using structural alignments with the UDP-galactose-4-epimerase UDP-glucose abortive complex (1XEL, 23) as a guide; no energy minimization was performed. The approximate placement of the glucopyranose moiety is constrained by the requirement for hydride transfer from C4 to NAD⁺, and from NADH back to C6. These constraints may necessitate a slightly different active site conformation, or a conformation change during chemistry, but Asp135 and Glu136 will always be adjacent to C6(OH), and Glu198 and Lys199 will be closer to C2(OH) and the pyrophosphate moiety. Ambiguities in the placement of the Glu198 side chain in the 4,6-dehydratase/NAD⁺ structure are represented by two overlapping ball-and-stick models, and indicated by lighter coloration. The stereoview was generated using Molview and PDB files 1XEL and 1BXK (23, 24).

for every reaction, a much slower, first-order (unsaturable) process.

The pH dependence of product C5 exchange and dTDP-6FGlc turnover catalyzed by wt 4,6-dehydratase are remarkably similar. Protonation of Glu136 negatively affects both of these processes, exhibiting a $pK_A \sim 6.6$ in both pH profiles. While a deprotonation event with a kinetic $pK_A \sim 9.4$ also affects catalysis, the identity of the deprotonated species is unknown. Candidates for this entity must be important for both reactions, and thus must be common elements, such as the thymidyl moiety of dTDP-sugars ($pK_A = 9.79$ free in solution; 25), or a residue similar to Lys199 and Glu198 that would perturb productive pyranose placement upon deprotonation.

As depicted in Scheme 2, product C5 solvent hydrogen exchange may result either from reversal of the last step in the catalytic mechanism (A) or from enolization (B). The absence of a significant deuterium isotope effect for abstraction of a hydride from C6 strongly suggests that product exchange is not occurring by reversal of the last step in turnover of dTDP-glucose. More likely, product exchange happens as a result of enolization as depicted in Scheme 2B. Because Tyr160 exists as the tyrosinate anion in the free enzyme at pH 7.5 ($pK_A = 6.4$; 9), it is unlikely that the Tyr160 is catalyzing enolization by protonating the C4 oxygen to form an enol, although C4 may be protonated by some other residue.

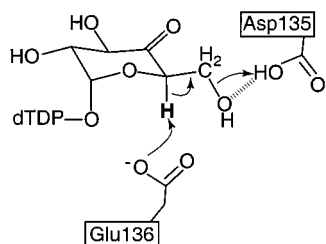
It is interesting to consider why k_{cat} and k_{cat}/K_M are 2 and 4 orders of magnitude lower with dTDP-6FGlc than with dTDP-glucose. During water elimination from dTDP-glucose, protonation of the leaving hydroxyl by Asp135 generates negative charge, which will not accumulate during fluoride elimination from dTDP-6FGlc, as Asp135 will remain protonated. Fluorine is otherwise an excellent substitution for a glucose hydroxyl group, resulting in minimal steric consequences, but covalently bonded fluorine is not capable of forming as many, or as strong, hydrogen bonds as is a hydroxyl group (26). This perhaps provides the basis for the

observed difference in turnover of dTDP-6FGlc and dTDP-glucose. The stereochemistry of water elimination by 4,6-dehydratase has been proposed to be syn (27), so presumably the enzyme provides some physical means to control the rotational freedom about the C5–C6 bond. This might result from steric conflicts, or from hydrogen-bonding interactions with the C6(OH). The slower rate for the dTDP-6FGlc turnover might result from the loss of this rotational control as fluorine is substituted for the hydroxyl.

This hypothesis initially appears to challenge the assignment of Asp135 as the acid catalyst for dehydration. Perhaps the Asp135 is not important for protonating the leaving group, but for tethering the C6(OH) in a conformation consistent with syn elimination. The importance of Asp135 as a tether vs an acid catalyst may be resolved by examining the rate constants for turnover of dTDP-glucose by the Asp135 variants (k_{cat} is 124- and 223-fold below wt for D135N and D135A, respectively, Table 1). If rotational control were the sole function of Asp135, one would see a much larger difference in activities of D135A and D135N variants, as D135N would still be capable of providing rotational control while D135A would not. Thus, the primary function of Asp135 is acid catalysis.

While this study unambiguously identifies Glu136 and Asp135 as the residues responsible for acid–base catalysis of dehydration, other aspects of the mechanism of this step are not well understood. Our previously suggested single-carboxylic acid model (7) is incompatible with our current panel of results, particularly the occurrence of C5 hydrogen exchange in the absence of water elimination. Scheme 4 shows our minimal model for the catalysis of water elimination using Glu136 and Asp135. This simple mechanism shows the direct action of these two residues in a concerted dehydration. A stepwise mechanism can also be imagined, where C5 is deprotonated, first forming an enolate (or enol) intermediate, which then eliminates water with protonation of the leaving hydroxyl. The concerted mechanism is attractive in its simplicity and avoids forming a high-energy

Scheme 4



intermediate. The stepwise mechanism is also compelling, particularly if one considers the potential participation of Tyr160 in protonating the enolate as it forms, generating the more stable enol and providing additional catalysis for dehydration. We are currently characterizing exchange reactions in ^{18}O -water to determine whether dehydration is stepwise or concerted.

ACKNOWLEDGMENT

We thank Professor W. W. Cleland for helpful advice and discussions. MALDI-TOF spectra were obtained at the University of Wisconsin–Madison Biophysics Instrumentation Facility, which is supported by the University of Wisconsin–Madison and Grants BIR-9512577 (NSF) and S10 RR13790 (NIH).

REFERENCES

- Liu, H.-W., and Thorson, J. S. (1994) *Annu. Rev. Microbiol.* 48, 223–256.
- Hutchinson, C. R. (1994) *Bio/Technology* 12, 375–380.
- Floss, H. G., Keller, P. J., and Beale, J. M. (1986) *J. Nat. Prod.* 49, 957–970.
- Marolda, C. L., and Valvano, M. A. (1995) *J. Bacteriol.* 177, 5539–5546.
- Rick, P. D., and Silver, R. P. (1996) *Escherichia coli and Salmonella Cellular and Molecular Biology* (Niedhardt, Ed.) 2nd ed., Vol. 1, pp 104–122, ASM Press, Washington, DC.
- Glaser, L., and Zarkowski, H. (1973) *The Enzymes* (Boyer, Ed.) Vol. 5, pp 465–480, Academic Press, New York.
- Hegeman, A. D., Gross, J. W., and Frey, P. A. (2001) *Biochemistry* 40, 6598–6610.
- Allard, S. T. M., Giraud, M.-F., Whitfield, C., Graninger, M., Messner, P., and Naismith, J. H. (2001) *J. Mol. Biol.* 307, 283–295.
- Gerratana, B., Cleland, W. W., and Frey, P. A. (2001) *Biochemistry* 40, 9187–9195.
- Jornvall, H., Persson, B., Krook, M., Atrian, S., Gonzalez-Duarte, R., Jeffery, J., and Ghosh, D. (1995) *Biochemistry* 34, 6003–6013.
- Liu, Y., Thoden, J. B., Kim, J., Berger, E., Gulick, A. M., Ruzicka, F. J., Holden, H. M., and Frey, P. A. (1997) *Biochemistry* 36, 10675–10684.
- Gabriel, O., and Lundquist, L. C. (1968) *J. Biol. Chem.* 243, 1479–1484.
- Melo, A., and Glaser, L. (1968) *J. Biol. Chem.* 243, 1475–1478.
- Gross, J. W., Hegeman, A. D., Vestling, M. M., and Frey, P. A. (2000) *Biochemistry* 39, 13633–13640.
- Stitt, B. L. (1988) *J. Biol. Chem.* 263, 11130–11137.
- Penefsky, H. S. (1977) *J. Biol. Chem.* 252, 2891–2899.
- Okazaki, R., Okazaki, T., Strominger, J. L., and Michelson, A. M. (1962) *J. Biol. Chem.* 237, 3014–3026.
- MacDonald, D. L. (1966) *Methods Enzymol.* 8, 121–125.
- Chang, C.-W. T., Chen, X. H., and Liu, H.-W. (1998) *J. Am. Chem. Soc.* 120, 9698–9699.
- Cleland, W. W. (1979) *Methods Enzymol.* 63, 102–138.
- Giraud, M.-F., and Naismith, J. H. (2000) *Curr. Opin. Struct. Biol.* 10, 687–696.
- Somoza, J. R., Menon, S., Schmidt, H., Joseph-McCarthy, D., Dessen, A., Stahl, M. L., Somers, W. S., and Sullivan, F. X. (2000) *Structure* 8, 123–135.
- Thoden, J. B., Frey, P. A., and Holden, H. M. (1996) *Biochemistry* 35, 5137–5144.
- Smith, T. J. (1995) *J. Mol. Graphics* 13, 122–125.
- Christensen, Rytting, and Izatt (1967) *J. Phys. Chem.* 71, 2700.
- Hoffmann, M., and Rychlewski, J. (2001) *J. Am. Chem. Soc.* 123, 2308–2316.
- Snipes, C. E., Brillinger, G. U., Sellers, L., Mascaro, L., and Floss, H. G. (1977) *J. Biol. Chem.* 252, 8113–8117.

BI011138C